

## Structural and Electrical Properties of SrRuO<sub>3</sub> thin Film Grown on SrTiO<sub>3</sub> (110) Substrate

O-Ung Kwon, Namic Kwon, B. W. Lee, and C. U. Jung \*

Department of Physics, Hankuk University of Foreign Studies, Yongin, Kyungki 449-791, Korea

(Received 17 January 2013, Received in final form 5 March 2013, Accepted 7 March 2013)

We studied the structural and electrical properties of SrRuO<sub>3</sub> thin films grown on SrTiO<sub>3</sub> (110) substrate. High resolution X-ray diffraction measurement of the grown film showed 1) very sharp peaks for SrRuO<sub>3</sub> film with a very narrow rocking curve with FWHM = 0.045° and 2) coherent growth behavior having the same in-plane lattice constants of the film as those of the substrate. The resistivity data showed good metallic behavior;  $\rho = 63$  (205)  $\mu\Omega\cdot\text{cm}$  at 5 (300) K with a residual resistivity ratio of  $\sim 3$ . The observed kink at  $\rho(T)$  showed that the ferromagnetic transition temperature was  $\sim 10$  K higher than that of SrRuO<sub>3</sub> thin film grown on SrTiO<sub>3</sub> (001) substrate. The observed rather lower RRR value could be partially due to a very small amount of Ru vacancy generally observed in SrRuO<sub>3</sub> thin films grown by PLD method and is evident in the larger unit-cell volume compared to that of stoichiometric thin film.

**Keywords :** SrRuO<sub>3</sub>, thin film, PLD, polar substrate, resistivity

### 1. Introduction

SrRuO<sub>3</sub> (SRO) is an itinerant ferromagnetic material and has attracted the attention of many researchers from  $\sim 1970$  [1]. Structurally, SRO is an end member of a well-known series of ruthenates Sr<sub>n+1</sub>Ru<sub>n</sub>O<sub>3n+1</sub> which includes a novel superconductor of Sr<sub>2</sub>RuO<sub>4</sub>. At low temperatures SRO is a Fermi liquid [2] while it exhibits bad metal behavior at high temperatures [3]. Due to its low resistivity and chemical stability, thin films of SRO have drawn tremendous interest as a conducting layer in epitaxial multilayered devices made of metal oxides, for example, as electrodes in oxide.

As previously studied, structural modification through to epitaxial strain in thin films modulates its magnetic properties significantly [4]. The SRO thin films have been grown most frequently on (001) plane of cubic substrate. Here, the in-plane compressive strain in SRO thin film grown coherently on SrTiO<sub>3</sub> (STO) (001) substrate pushes the magnetic easy axis normal to the surface direction and suppressed  $T_c$  to about 150 K [4]. Previously, we demonstrated the trends of inherently lower lattice mismatch of an orthorhombic crystal along the cubic substrate [1-10]

in-plane direction than along the cubic substrate [001] in-plane direction [5]. Here, we deposited SRO on STO (110) substrate to study the structural and electrical properties of the film. The lattice constants of SRO are  $a = 5.567$  ( $3.936 \times \sqrt{2}$ ) Å,  $b = 5.5304$  ( $3.9106 \times \sqrt{2}$ ) Å, and  $c = 7.8446$  ( $3.9223 \times 2$ ) Å and those for STO in 'pseudo-orthorhombic' notation are  $a = b = 5.523$  ( $3.905 \times \sqrt{2}$ ) Å,  $c = 7.81$  ( $3.905 \times 2$ ) Å. Note that we used pseudo-cubic lattice notation for SRO for easy comparison.

### 2. Experimental

SRO thin films were grown by using a pulsed laser deposition method with KrF excimer laser pulses of 36 mJ (measured just before laser window) focused on a stoichiometric ceramic target [5-8]. For simplicity, we will use "SRO<sub>001</sub>film" and "SRO<sub>110</sub>film," for the SRO film grown on STO (001) substrate and STO (110) substrate, respectively. The substrate was in-situ annealed at 950°C at  $10^{-7}$  Torr for 5 minutes. The films were grown  $T \sim 750$  °C and oxygen partial pressure during the growth was approximately  $\sim 100$  mTorr. Reflection high-energy electron diffraction was used for in-situ monitoring of the surface during the growth of film. The typical thickness for the grown films was 30 nm. The crystal structure of the grown films was identified by using a high-resolution X-ray diffractometer having Cu-k $_{\alpha}$  radiation and transport

©The Korean Magnetism Society. All rights reserved.

\*Corresponding author: Tel: +82-31-330-4952

Fax: +82-31-330-4566, e-mail: cu-jung@hufs.ac.kr

properties of the films were obtained by using a physical property measurement system (PPMS, Quantum Design).

### 3. Results and Discussion

Figure 1(a) shows the RHEED image of STO (110) substrate after 5 minutes in-situ annealing under  $T = 950^\circ\text{C}$  at  $10^{-7}$  Torr inside the PLD chamber. The brightest spot within the white box clearly shows that the surface of the substrate is atomically flat. However, the surface became rough as soon as SRO thin film grew. The rectangular array of white spots in Fig. 1(b) shows the island growth mode. This growth mode is in sharp contrast with the step-flow mode observed in the SRO film grown on top of STO (001) substrate [5]. While there was a model that attempted to rationalize the diverse growth modes observed in the PLD of SRO on STO (001) substrates, the existence of the highly polar stacking layer of SrTiO<sup>4+</sup> or O<sub>2</sub><sup>4-</sup> in the STO (110) surface may be another factor to avoid the step flow mode [9, 10].

Even though the surface of the *SrRuO<sub>3</sub> film* is not as perfect as that of SRO thin film grown on STO (001) substrate whose stacking layer is electrically neutral, the quality of crystallinity was the same as that of SRO thin film grown on STO (001) substrate. There was a strong

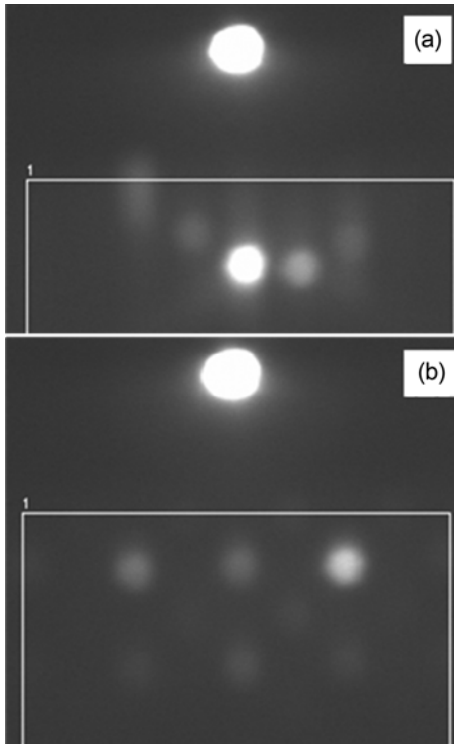


**Fig. 1.** (a) RHEED pattern of SrTiO<sub>3</sub> (110) substrate just before film growth, (b) RHEED pattern of the SrRuO<sub>3</sub> film after three minutes' growth.

SRO film peak near  $2\theta = 31.988^\circ$  together with the strongest substrate peak near  $2\theta = 32.400^\circ$ . The calculated lattice constant of the *SrRuO<sub>3</sub> film* was  $d_{110} = 2.7956 \text{ \AA} = (3.954 \pm 0.001) \text{ \AA} / \sqrt{2}$  which is a quite reasonable value [7]. The quality of the film was also identified by the very narrow rocking curve widths of  $0.045^\circ$  for the SRO (110)c peak. [We use pseudo-cubic notation for SRO.]

To obtain the in-plane lattice constants, we measured the X-ray reciprocal space mapping around the STO (400) plane and the STO (222) plane. The X-ray reciprocal space mapping in Fig. 3 shows strong film peaks in the lower region and two very strong substrate peaks in the upper region. The clear separation of the film peaks corresponding to Cu  $\kappa\alpha_1$  and  $\kappa\alpha_2$  radiation means that the in-plane coherent epitaxial growth of the *SrRuO<sub>3</sub> film* is excellent along both the STO [1-10] in-plane direction and the STO [001] in-plane direction. The obtained  $d_{220}$  values for the *SrRuO<sub>3</sub> film* were consistent with the  $d_{110}$  values obtained in the  $\theta$ - $2\theta$  scan in Fig. 2. The positions of the film peaks along the horizontal axis are the same as those of substrate peaks, which means that the *SrRuO<sub>3</sub> film* was grown fully coherently along both in-plane direc-

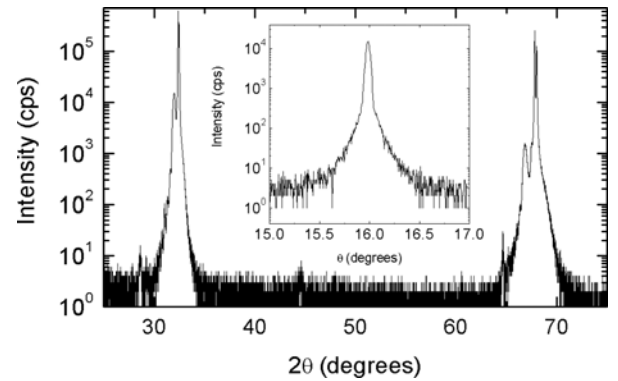


**Fig. 2.** High resolution X-ray  $\theta$ - $2\theta$  scan for the SrRuO<sub>3</sub> thin film on SrTiO<sub>3</sub> (110) substrate. Inset shows rocking curve for SrRuO<sub>3</sub> film (110)c peak.

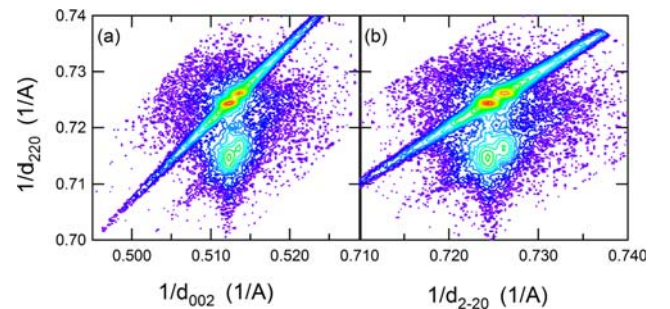


**Fig. 3.** (Color online) X-ray reciprocal space mapping around STO (222) and (400) planes of the SrRuO<sub>3</sub> thin film on SrTiO<sub>3</sub> (110) substrate.

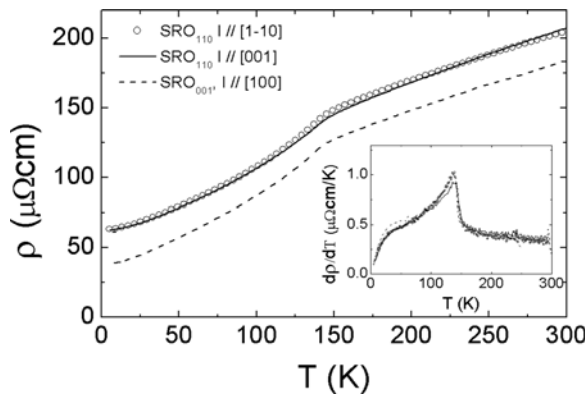


**Fig. 4.** Resistivity curve for the SrRuO<sub>3</sub> thin film on SrTiO<sub>3</sub> (110) substrate with two current directions. For comparison, the resistivity curve for the SrRuO<sub>3</sub> thin film on SrTiO<sub>3</sub> (001) substrate with current direction along the in-plane direction is also shown.

tions, having the same in-plane lattice constants;  $d_{1-10} = 3.905/\sqrt{2}$  Å and  $d_{002} = 3.905/2$  Å as those of STO (110) substrate. This also indicates that the films are under compressive strain along both in-plane directions while the amount of strain is different from each other [5, 7, 8]. Combining the HRXRD data, we can calculate the unit cell volume of the *SRO<sub>110</sub> film*;  $V_{\text{pseudocubic}} = 3.905^2 \times 3.954$  Å<sup>3</sup> = 3.921<sup>3</sup> Å<sup>3</sup>. The volume is smaller than that of bulk SRO, which is generally explained by the effect of compressive strain.

Figure 4 presents the temperature dependence for the resistivity of the *SRO<sub>110</sub> film*. For the *SRO<sub>110</sub> film*, the room temperature resistivity was  $\rho(300 \text{ K}) \sim 205$  μΩ·cm and the resistivity at 5 K was  $\sim 63$  μΩ·cm with a residual resistivity ratio (RRR) of 3. While the resistivity at low temperatures was higher than expected, the upturn of resistivity at low temperatures observed for other group's SRO films was not observed in our *SRO<sub>110</sub> film* [11]. The kink in the resistivity near 160 K is known to be caused by the ferromagnetic transition temperature. For comparison we inserted  $\rho(T)$  of *SRO<sub>001</sub> film*. So, the ferromagnetic transition temperature of the *SRO<sub>110</sub> film* is a little bit higher than that of the *SRO<sub>001</sub> film* grown on STO (001) substrate. [We also plotted the  $d\rho/dT$  curve where main peak is related to ferromagnetic transition.] This difference can be explained by the smaller lattice mismatch which becomes available by adopting (110) plane of cubic substrate instead of (001) plane to grow orthorhombic crystal [5, 7, 8]. With orthorhombic *a*-axis growth of the SRO film on a STO (110) substrate, the mismatch along the STO [1-10] in-plane direction is lower than that along the STO [001] in-plane direction. Moreover, these mismatches are smaller than those observed in SRO film grown on

STO (001) substrate.

The overall resistivity value for the *SRO<sub>110</sub> film* was higher than that for the *SRO<sub>001</sub> film*, especially at low temperatures. The unit cell volume of the *SRO<sub>110</sub> film* was  $3.905^2 \times 3.955 = 3.921^3$  Å<sup>3</sup> in pseudo-cubic notation which is smaller than that of bulk. However, unit cell volume 241.18 Å<sup>3</sup> in orthorhombic notation is larger than that of cation stoichiometric film [12]. Siemons *et al.*, estimated that the Ru vacancy concentration causing drastic change of RRR is much smaller than a few percent for the range of samples they studied, from the fact that the decrease of curie temperature is as small as  $\sim 10$  K [12]. According to the recent review paper, this volume expansion came from Ru vacancy and gives a smaller RRR value. However, the orthorhombic volume 241.18 Å<sup>3</sup> corresponds to RRR  $\sim 10$  in the paper and our RRR value is three times smaller than that. So, simple explanation in terms of a structural factor such as volume expansion is not enough to explain different RRR values even though we accept that PLD grown SRO films have a greater tendency to have larger lattice volume and lower RRR values [12].

## 4. Conclusions

We studied the structural and electrical properties of SrRuO<sub>3</sub> thin films grown on SrTiO<sub>3</sub> (110) substrate. While the surface of the film was not as perfectly flat as that of SrRuO<sub>3</sub> thin films grown on SrTiO<sub>3</sub> (001) substrate, the quality of crystallinity was the same as that of SrRuO<sub>3</sub> thin films grown on SrTiO<sub>3</sub> (001) substrate. The resistivity data showed good metallic behavior, but with a rather smaller value of residual resistivity ratio of  $\sim 3$ . The lower RRR value could be partially due to the minimal amount of Ru vacancy generally observed in PLD grown SrRuO<sub>3</sub> thin films.

## Acknowledgment

C. U. Jung was supported by the Hankuk University of Foreign Studies Research Fund of 2012. O-Ung Kwon and B. W. Lee were supported by the Basic Science Research Program through the National Research Foundation of Korea (NRF) funded by the Ministry of Education, Science and Technology (2012R1A1A2008845).

## References

- [1] G. Koster, L. Klein, W. Siemons, G. Rijnders, J. S. Dodge, C. B. Eom, D. H. A. Blank, and M. R. Beasley, *Rev. Mod. Phys.* **84**, 253 (2012).
- [2] A. P. Mackenzie, J. W. Reiner, A. W. Tyler, L. M. Galvin,

- S. R. Julian, M. R. Beasley, T. H. Geballe, and A. Kapitulnik, *Phys. Rev. B* **58**, R13, 318 (1998).
- [3] L. Klein, J. S. Dodge, C. H. Ahn, J. W. Reiner, L. Mieville, T. H. Geballe, M. R. Beasley, and A. Kapitulnik, *J. Phys.: Condens. Mater* **8**, 10111 (1996).
- [4] Q. Gan, R. A. Rao, C. B. Eom, J. L. Garrett, and Mark Lee, *Appl. Phys. Lett.* **72**, 978 (1998).
- [5] B. W. Lee and C. U. Jung *J. Kor. Phys. Soc.* **6**, 795 (2012).
- [6] C. U. Jung, H. Yamada, M. Kawasaki, and Y. Tokura, *Appl. Phys. Lett.* **84**, 2590 (2004).
- [7] B. W. Lee and C. U. Jung, *J. Kor. Phys. Soc.* **59**, 322 (2011).
- [8] B. W. Lee and C. U. Jung, *Appl. Phys. Lett.* **96**, 102507 (2010).
- [9] W. Hong, H. N. Lee, M. Yoon, H. M. Christen, D. H. Lowndes, Z. Suo, and Z. Zhang, *Phys. Rev. Lett.* **95**, 095501 (2005).
- [10] M. Yoon, H. N. Lee, W. Hong, H. M. Christen, Z. Zhang, and Z. Suo, *Phys. Rev. Lett.* **99**, 055503 (2007).
- [11] M. A. Lopez de la Torre, Z. Sefroui, D. Arias, M. Varela, J. E. Villegas, C. Ballesteros, C. Leon, and J. Santamaria, *Phys. Rev. B* **63**, 052403 (2001).
- [12] W. Siemons, G. Koster, A. Vailionis, H. Yamamoto, D. H. A. Blank, and M. R. Beasley, *Phys. Rev. B* **76**, 075126 (2007).